SPARSE REPRODUCING KERNELS FOR MODELING FIBER CROSSINGS IN DIFFUSION WEIGHTED IMAGING

Cory Ahrens, Jennifer Nealy

Applied Mathematics and Statistics
Colorado School of Mines
Golden, CO 80401

Fernando Pérez, Stéfan van der Walt

Helen-Wills Neuroscience Institute
University of California, Berkeley
Berkeley, CA 94720

ABSTRACT

Using existing estimators found in High Angular Resolution Diffusion Imaging (HARDI), such as the Orientation Probability Distribution Function (OPDF) of Aganj *et al*., we develop a new mathematical framework for implementing HARDI. In contrast to traditional methods based on spherical harmonics, the framework is based on a reproducing kernel formalism combined with recently developed Gaussian-like quadratures for the sphere, which leads to an efficient and sparse representation for HARDI estimators. We demonstrate that the new framework results in reconstructions that are more robust to noise and have better angular resolution, compared to spherical harmonic based reconstructions.

1. INTRODUCTION

Based on the classical work of Stejskal and Tanner [11], diffusion magnetic resonance imaging (dMRI) has become a key tool in understanding complex structural aspects of white matter in the brain. With measurement techniques improving, initial reconstruction algorithms such as Diffusion Tensor Imaging (DTI) were shown to be limited in their ability to resolve complex structures. This lead to a class of algorithms known as High Angular Resolution Diffusion Imaging (HARDI), which aims primarily to reconstruct angular information about underlying neural structures. Because of restricted diffusion of water molecules along these structures, angular information is typically localized to certain directions. Thus, within the HARDI framework, there is need to develop reconstruction algorithms that can accurately and efficiently capture localized angular information. We present the initial development of such an algorithm in this paper.

2. THEORY AND METHODS

Signal attenuation $S(\mathbf{q};\tau)$ can be related to the ensemble average probability that a spin will diffuse a displacement $\mathbf{r} = \mathbf{x} - \mathbf{x}_0$, relative to position $\mathbf{x}_0$, during a diffusion time τ by the Fourier relationship $S(\mathbf{q};\tau) = S_0\mathcal{F}[P(\mathbf{r};\tau)](\mathbf{q})$, where $\mathcal{F}$ is the 3-D Fourier transform, $\mathbf{q} = \gamma\delta\mathbf{G}/2\pi$, γ is the nuclear gyromagnetic ratio for protons in water, δ is the pulse duration, $\mathbf{G}$ is the applied diffusion gradient vector and $P(\mathbf{r};\tau)$ is the ensemble average propagator (EAP) [7]. The gradient free signal is denoted by S_0. To invert the Fourier transform all of 3-D q-space must be sampled. This is typically too costly for clinical applications and hence various approximations have been developed (see e.g. [4]). One such approximation technique is HARDI.

HARDI techniques recover angular information about the EAP through its radial integral. While different definitions for the integration exist, we choose to follow the approach of [1], since their formulation correctly accounts for the spherical r^2 weighting in the radial integral. With this weighting, one arrives at the Orientation Probability Distribution Function (OPDF), which can be interpreted as a marginal probability distribution.

A common feature of HARDI techniques is the need to recover from a set of noisy measurements a function defined on the unit sphere that exhibits localized behavior. Traditionally, spherical harmonics have been used to represent functions on the sphere, but because of their global nature they are not efficient at representing functions with localized features. We remark that the framework we develop has similarities to the work of [9, 13], but with important differences discussed below.

2.1. Preliminaries

Since the OPDF is defined on the unit sphere $\mathbb{S}^2$, a natural starting point for its recovery are the spherical harmonics—an orthonormal basis for the space of square integrable functions on the sphere, $L^2(\mathbb{S}^2)$. Here, we simply collect relevant properties of spherical harmonics which can be found in, e.g., [5]. A spherical harmonic of degree l and order m is defined by $Y_l^m(\theta,\phi) = (-1)^m c_l^m P_l^m(\cos\theta)\, e^{im\phi}$, where $P_l^m(\mu)$ is the Associated Legendre function, the normalization constant $c_l^m = \sqrt{\frac{(2l+1)(l-m)!}{4\pi(l+m)!}}$ and $-l \le m \le l$. Here, $0 \le \theta < \pi$ is the polar angle and $0 \le \phi < 2\pi$ is the azimuthal angle. Spherical harmonics satisfy the Addition Theorem, which states that for $\mathbf{\Omega}, \mathbf{\Omega}' \in \mathbb{S}^2$,

$\frac{2l+1}{4\pi} P_l\left(\boldsymbol{\Omega}\cdot\boldsymbol{\Omega}'\right) = \sum_{|m|\le l} \bar{Y}_l^m\left(\boldsymbol{\Omega}'\right) Y_l^m\left(\boldsymbol{\Omega}\right)$, where $P_l\left(\mu\right)$ the l^{th} degree Legendre polynomial and the over-bar denotes complex conjugation. In addition, spherical harmonics are eigenfunctions of the Laplace-Beltrami operator on the sphere: $\Delta_b Y_l^m\left(\theta,\phi\right) = -l\left(l+1\right) Y_l^m\left(\theta,\phi\right)$. Moreover, the so-called Funk-Hecke Theorem states that spherical harmonics are eigenfunctions for a particular integral operator on the sphere with kernel $f\left(\mu\right)$ defined on $[-1,1]$, that is, $\int_{\mathbb{S}^2} f\left(\boldsymbol{\Omega}\cdot\boldsymbol{\Omega}'\right) Y_l^m\left(\boldsymbol{\Omega}'\right) d\boldsymbol{\Omega}' = \lambda_l Y_l^m\left(\boldsymbol{\Omega}\right)$, where $\lambda_l = 2\pi\int_{-1}^{1} f\left(\mu\right) P_l\left(\mu\right) d\mu$ is the eigenvalue. This can be used to find the action of the so-called Funk-Radon transform $\mathcal{G}f\left(\mathbf{u}\right) = \int_{\mathbb{S}^2} \delta\left(\mathbf{u}\cdot\mathbf{v}\right) f\left(\mathbf{v}\right) d\mathbf{v}$, when f is a linear combination of spherical harmonics.

2.1.1. Approximation on $\mathbb{S}^2$

To develop a framework in which to approximate the OPDF, we start with a subspace of spherical harmonics of maximum degree L: $\mathcal{H}_L = \text{span}\left\{Y_l^m\left(\boldsymbol{\Omega}\right) : |m| \le l,\, 0 \le l \le L\right\}$. If $f \in \mathcal{H}_L$, then f can be written as $f = \sum_{l=0}^{L}\sum_{|m|\le l} f_l^m Y_l^m$, where $f_l^m = \int_{\mathbb{S}^2} \bar{Y}_l^m\left(\boldsymbol{\Omega}\right) f\left(\boldsymbol{\Omega}\right) d\Omega$ is the spherical harmonic coefficient of f. Substituting the definition of f_l^m into this expansion, interchanging summation and integration and using the Addition Theorem, we arrive at the reproducing identity [3]

$$f\left(\boldsymbol{\Omega}\right) = \int_{\mathbb{S}^2} K\left(\boldsymbol{\Omega}\cdot\boldsymbol{\Omega}'\right) f\left(\boldsymbol{\Omega}'\right) d\boldsymbol{\Omega}', \text{ for all } f \in \mathcal{H}_L, \quad (1)$$

with $K\left(\mu\right) = \sum_{l=0}^{L} \frac{2l+1}{4\pi} P_l\left(\mu\right)$ the reproducing kernel for $\mathcal{H}_L$. It can be shown that the operator $\int_{\mathbb{S}^2} K\left(\boldsymbol{\Omega}\cdot\boldsymbol{\Omega}'\right)\left(\cdot\right) d\boldsymbol{\Omega}'$ is a projector from $L^2\left(\mathbb{S}^2\right)$ onto $\mathcal{H}_L$ [5]. Because of inherent symmetry in dMRI, we project onto only the even harmonics in $\mathcal{H}_L$ by using

$$K_e\left(\mu\right) \equiv \sum_{l=0}^{\lfloor L/2\rfloor} \frac{4l+1}{4\pi} P_{2l}\left(\mu\right), \quad (2)$$

where $\lfloor n\rfloor$ is the greatest integer less than n, as the kernel in Eq. (1). Thus, to reconstruct an OPDF we use the representation Eq. (1) with kernel Eq. (2). For reasons explained below, in the sequel we start the sum in Eq. (2) at $l = 2$ to explicitly remove any constant term from f. To develop a computational algorithm based on Eq. (1), we now discretize the integral using newly developed quadratures for the sphere.

2.1.2. Quadratures

While quadratures for Cartesian domains are relatively well developed, research in quadratures for the sphere remains an active area of research [5]. The difficulty in developing such quadratures, and hence associated sampling algorithms, arises because of the topology of the sphere. This is reflected in the fact that at most only 20 points can be uniformly distributed on the sphere. Said differently, a set of 21 or more points on the sphere must necessarily be unevenly distributed. Moreover, while Gaussian quadratures for Cartesian domains exist and are well known, it was only recently proven that Gaussian quadratures for the sphere do not, in fact, exist [6].

To develop an efficient sampling scheme by discretizing Eq. (1), we rely on recently developed, Gaussian-like quadratures from [2]. Unlike other approaches, these new quadratures are invariant under icosahedral rotations and hence do not cluster. More importantly, they are highly efficient (nearly Gaussian) and exactly integrate subspaces of spherical harmonics. In fact, to represent functions in $\mathcal{H}_L$ one needs (asymptotically) only $\sim 4L^2/3$ points. See [2] for more details.

Let $\{\boldsymbol{\Omega}_i, w_i\}_{i=1}^{M}$ denote a quadrature that exactly integrates functions of degree at least $2L$. Here $\boldsymbol{\Omega}_i \in \mathbb{S}^2$ is a quadrature point with associated weight w_i. From Eq. (1) we have the representation $f\left(\boldsymbol{\Omega}\right) = \sum_{i=1}^{M} f\left(\boldsymbol{\Omega}_i\right) w_i K_e\left(\boldsymbol{\Omega}\cdot\boldsymbol{\Omega}_i\right)$. This is an exact representation for even functions in $\mathcal{H}_L$ and is analogous to Lagrange interpolation in that f is a linear combination of function values and a single function K_e.

2.1.3. Signal representation

Aganj *et al.* [1] showed that the OPDF $\Phi\left(\boldsymbol{\Omega}\right) = \int_0^\infty P\left(r\boldsymbol{\Omega};\tau\right) r^2 dr$ can be approximated by

$$\Phi\left(\boldsymbol{\Omega}\right) \approx \frac{1}{4\pi} + \frac{1}{16\pi^2}\mathcal{G}\left\{\Delta_b \ln\left(-\ln\, S\left(\mathbf{q}\right)\right)\right\}\left(\boldsymbol{\Omega}\right), \quad (3)$$

where a mono-exponential model was assumed for the radial dependence of P. The constant term, $1/4\pi$, represents the isotropic component of $\Phi\left(\boldsymbol{\Omega}\right)$, while the second term describes any angular variation in $\Phi\left(\boldsymbol{\Omega}\right)$. Because of the Funk-Radon and the Laplace-Beltrami operators, the second term is an even function of $\boldsymbol{\Omega}$ and does not contain any constant terms, and is the reason we start the sum in Eq. (2) at $l = 2$.

The shape of the reproducing kernel $K_e\left(\mu\right)$ suggests that the OPDF should have a sparse representation in terms of linear combinations of the kernels K_e and hence we set

$$\Phi\left(\boldsymbol{\Omega}\right) \approx \frac{1}{4\pi} + \sum_{i=1}^{M} \Phi_i K_e\left(\boldsymbol{\Omega}\cdot\boldsymbol{\Omega}_i\right) \quad (4)$$

where the coefficients $\{\Phi_i\}_{i=1}^{M}$ will be determined by the diffusion signal S at $\{\mathbf{q}_i\}_{i=1}^{N}$ gradient directions. An important property of the representation Eq. (4) is that peaks (maxima) in Φ can be easily identified by considering dominant coefficients Φ_i, since $K_e\left(\boldsymbol{\Omega}\cdot\boldsymbol{\Omega}_i\right)$ is peaked in direction $\boldsymbol{\Omega}_i$. In order to determine the coefficients in Eq. (4), we set, once the mean of the signal S has been removed, for $i = 1, 2, ...N$

$$\ln\left(-\ln\, S\left(\mathbf{q}_i\right)\right) = \sum_{j=1}^{M} \Phi_j H_e\left(\boldsymbol{\Omega}_i\cdot\boldsymbol{\Omega}_j\right), \quad (5)$$

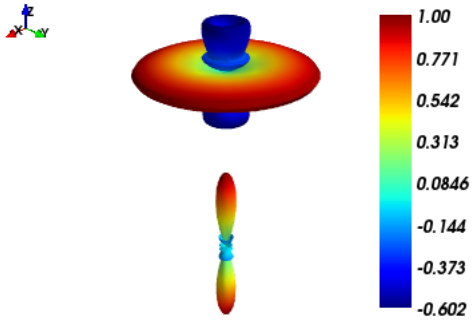

Fig. 1. Kernels Eq. (2) (bottom) and Eq. (6) (top) for $L = 8$ and starting at $l = 2$.

where we define

$$H_e\left(\mathbf{\Omega}\cdot\mathbf{\Omega}_i\right) \equiv -\frac{1}{16\pi^2}\sum_{l=2}^{\lfloor L/2\rfloor}\frac{4l+1}{l\left(2l+1\right)P_{2l}\left(0\right)}P_{2l}\left(\mathbf{\Omega}\cdot\mathbf{\Omega}_i\right). \tag{6}$$

By construction $\mathcal{G}\left\{\Delta_b H_e\left(\mathbf{\Omega}\cdot\mathbf{\Omega}_i\right)\right\} = K_e\left(\mathbf{\Omega}\cdot\mathbf{\Omega}_i\right)$ and, hence, solving Eqs. (5) for $\{\Phi_i\}_{i=1}^{M}$ yields Eq. (4) . The relationship $\mathcal{G}\left\{\Delta_b H_e\left(\mathbf{\Omega}\cdot\mathbf{\Omega}_i\right)\right\} = K_e\left(\mathbf{\Omega}\cdot\mathbf{\Omega}_i\right)$ can be verified using the Addition Theorem, the Funk-Hecke formula, the Funk-Radon transform and the fact that the spherical harmonics are eigenfunctions of the Laplace-Beltrami operator. Fig. 1 shows a plot of $K_e\left(\mathbf{\Omega}\cdot\hat{e}_z\right)$ as well $H_e\left(\mathbf{\Omega}\cdot\hat{e}_z\right)$ for degree $L = 8$ with $\hat{e}_z$ the unit vector pointing in the positive z direction. We see that K_e is peaked in the directions $\hat{e}_z$ and $-\hat{e}_z$ and decays rapidly. The function $H_e\left(\mathbf{\Omega}\cdot\hat{e}_z\right)$ is peaked along the great circle whose normal is perpendicular to $\hat{e}_z$.

We have in mind the case where $N \ll M$, that is, we have many fewer measurements than coefficients and hence Eq. (5) is an under-determined system. Guided by compressive sensing techniques [8], we regularize the system by solving the minimization problem

$$\min_{\Phi_i}\frac{1}{2N}\left\|\mathbf{H\Phi}-\mathbf{S}\right\|_2^2+\alpha\rho\left\|\mathbf{\Phi}\right\|_1+\frac{\alpha\left(1-\rho\right)}{2}\left\|\mathbf{\Phi}\right\|_2^2, \tag{7}$$

where α and ρ are regularization parameters. We use the elastic net solver in the Python software package scikit-learn [10] to solve Eq. (7). These coefficients are then used in Eq. (4) to represent Φ.

As noted earlier, significant coefficients Φ_i correspond to directions in the quadrature set $\mathbf{\Omega}_i$ near OPDF peaks. These directions can therefore be used as starting positions for finding peaks in the OPDF.

3. RESULTS

To validate the above framework, we simulated recovering the angle of two crossing fibers, the dMRI signal of which can be modeled as the sum of two Gaussians with equal volume fraction. Specifically, a synthetic signal was generated using $S\left(\mathbf{g}\right) = \left(e^{-b\,\mathbf{g}^T\mathbf{D}_1\mathbf{g}}+e^{-b\,\mathbf{g}^T\mathbf{D}_2\mathbf{g}}\right)/2$, where $\mathbf{D}_1 = \mathrm{diag}\left(\lambda_1,\lambda_2,\lambda_3\right)$, $\lambda_1 = 1800\times10^{-6}\,\mathrm{mm/s^2}$, $\lambda_2 = \lambda_3 = 200\times10^{-6}\,\mathrm{mm/s^2}$ is the diffusion tensor, $\mathbf{D}_2$ is a rotated version of $\mathbf{D}_1$, and $b = 3000\,\mathrm{s/mm^2}$. To the signal we added Rician noise at a level of $\mathrm{PSNR} = 20$, with PSNR defined to be S_m/σ, with $S_m = 1$ the signal maximum and σ the standard deviation of the Gaussian noise components. To test the method's angular resolution, the crossing angle was increased from 30 to 90 degrees. At each crossing angle, the signal was sampled at $N = 64$ locations, corresponding to a set of electrostatic repulsion directions found in Siemens scanners.

With $L = 10$, a quadrature from [2] with $M = 192$ that exactly integrates spherical harmonics of maximum degree 23, was used to create the 192 functions using Eq. (6). The minimization problem Eq. (7) was then solved for the coefficients Φ_i. We found empirically that $\alpha = 5\times10^{-4}$ and $\rho = 0.99$ worked well. With these coefficients determined, peaks in Eq. (4) were found by comparing OPDF values in 10242 positions on the sphere, obtained by subdivision of the unit icosahedron. The estimated fiber crossing angle was taken to be the angle between peaks in Eq. (4).

We compared our method with reconstructions based on [1], which yielded best results using spherical harmonics of maximum degree 6, as suggested by [12]. Note that the method presented in this paper is essentially that of [1], but using sparsely fit localized functions from Eq. (6) instead of spherical harmonics, centered at appropriately chosen locations (quadrature points) on the sphere.

Results, summarizing 50 attempts at recovering each crossing angle, are shown in Fig. (2). Note that the reconstruction algorithm outlined above (hereafter referred to as the sparse kernel algorithm) results in significantly better angular resolution when the crossing angle is between 30° and approximately 45°. For crossing angles greater than approximately 45°, the spherical harmonics based algorithms and sparse kernel algorithm have approximately the same average angular error.

4. DISCUSSION

We have presented the initial development of a framework in which HARDI estimators can be reconstructed. This framework is based on the reproducing kernel structure for subspaces of spherical harmonics and efficient quadratures for the sphere. Because of oversampling, we are able to achieve localization of the basis functions, Eq. (6), in contrast to spherical harmonics. Moreover, because HARDI signals typically have localized features, these new functions better match the signal and hence we are able to achieve better angular resolution.

There are similarities between the algorithm in this paper and those found in [9, 13], which are based on spherical wavelets. Because of our use of efficient, Gaussian-like

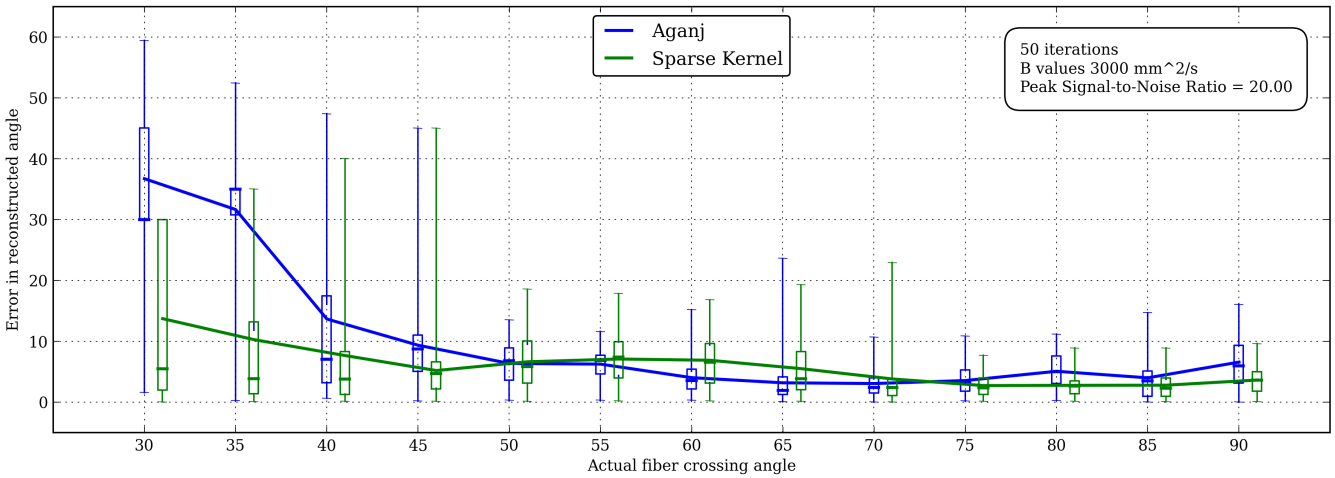

Fig. 2. Results of a Monte Carlo simulation estimating the angle between two fibers, based on the OPDF recovered respectively by [1] and this paper (*sparse kernel model*). The solid lines represent error means, while the box plots indicate first and third error quartiles (box) and outliers (whiskers).

quadratures, fewer basis functions are required, resulting in a more efficient algorithm. Moreover, because of the use of exact quadratures and the reproducing kernel framework, we can say precisely in what subspace our reconstructed signal lies.

We plan to further develop and test the algorithm against various other approaches and report results in a future publication. The code and data needed to reproduce this paper are publicly available at `http://bit.ly/ahrens_etal_ISBI2013`.

Acknowledgments The authors would like to thank B. Amirbekian, A. Rokem and E. Garyfallidis for their contributions to the Diffusion Imaging in Python project (`http://dipy.org`) on which our work is built.

5. REFERENCES

[1] I. Aganj et al. Reconstruction of orientation distribution function in single- and multi-shell q-ball imaging within constant solid angle. *Magn. Reson. Med.*, 64:554–566, 2010.

[2] C. Ahrens and G. Beylkin. Rotationally invariant quadratures for the sphere. *Proc. Roy. Soc. A*, 465:3103–3125, 2009.

[3] A. Aronszajn. Theory of reproducing kernels. *Trans. Amer. Math. Soc.*, 68(3):337–404, 1950.

[4] H. Assemlala et al. Recent Advances in Diffusion MRI Modeling: Angular and Radial Reconstruction. *Med. Image Anal.*, 15(4):369–96, 2011.

[5] K. Atkinson and W. Han. *Spherical Harmonics and Approximations on the Unit Sphere: An Introduction*. LNM 2044. Springer, 2012.

[6] E. Bannai and E. M. Damerell. Tight spherical designs, I. *J. Math Soc. Jap.*, 31:199–207, 1979.

[7] P.T. Callahan. *Principles of Nuclear Magnetic Resonance Miscroscopy*. Clarendon Press., Oxford, 1991.

[8] Y. C. Eldar and G. Kutyniok. *Compressed Sensing: Theory and Applications*. Cambridge University Press, 2012.

[9] O. Michailovich and Y. Rathi. Fast and accurate reconstruction of HARDI data using compressed sensing. *Med. Image. Comput. Comput. Assist. Interv.*, 13:607–614, 2010.

[10] F. Pedregosa et al. Scikit-learn: Machine Learning in Python . *Journal of Machine Learning Research*, 12:2825–2830, 2011.

[11] E. O. Stejskal and J. E. Tanner. Spin diffusion measurements: spin echoes in the presence of a time-dependent field gradient. *J. Chem. Phys.*, 42(1):288–292, 1965.

[12] A. Tristán-Vega et al. A new methodology for the estimation of fiber populations in the white matter of the brain with the Funk-Radon transform. *NeuroImage*, 49:1301–1315, 2010.

[13] A. Tristán-Vega and C. Westin. Probabilistic ODF estimation from reduced HARDI data with sparse regularization. In A. Martel and T. Peters G. Fichtinger, editor, *MICCAI 2011: Part II*, pages 182–190, 2011.